University of Zurich[UZH]

Zurich Open Repository and Archive
University of Zurich
Main Library
Strickhofstrasse 39
CH-8057 Zurich
www.zora.uzh.ch

Year: 2012

Synthesis and acid-Base properties of an imidazole-containing nucleotide analog, 1-(2'-Deoxy-B-D-ribofuranosyl)imidazole 5'-monophosphate (dImMP2-)

Megger, N ; Johannsen, S ; Mueller, J ; Sigel, Roland K O

Abstract: Deletion of the substituted pyrimidine ring in purine-2'-deoxynucleoside 5'-monophosphates leads to the artificial nucleotide analog dImMP(2-). This analog can be incorporated into DNA to yield, upon addition of Ag+ ions, a molecular wire. Here, we measured the acidity constants of H-2(dImMP)(+/-) having one proton at N(3) and one at the PO32- group by potentiometric pH titrations in aqueous solution. The micro acidity constants show that N(3) is somewhat more basic than PO32- and, consequently, the (H center dot dImMP)(-) tautomer with the proton at N(3) dominates to ca. 75%. The calculated micro acidity constants are confirmed by P-31- and H-1-NMR chemical shifts. The assembled data allow many quantitative comparisons, e.g., the N(3)-protonated and thus positively charged imidazole residue facilitates deprotonation of the P(O)(2)(OH)- group by 0.3 pK units. Information on the intrinsic site basicities also allows predictions about metal-ion binding; e.g., Mg2+ and Mn2+ will primarily coordinate to the phosphate group, whereas Ni2+ and Cu2+ will preferably bind to N(3). Macrochelate formation for these metal ions is also predicted. The micro acidity constant for N(3)H+ deprotonation in the (H center dot dImMP center dot H)(+/-) species (pk(a) 6.46) and the Mn+-binding properties are of relevance for understanding the behavior of dImMP units present in DNA hairpins and metalated duplexes.

DOI: https://doi.org/10.1002/cbdv.201100437

Posted at the Zurich Open Repository and Archive, University of Zurich
ZORA URL: https://doi.org/10.5167/uzh-75257
Journal Article
Published Version

Originally published at:
Megger, N; Johannsen, S; Mueller, J; Sigel, Roland K O (2012). Synthesis and acid-Base properties of an imidazole-containing nucleotide analog, 1-(2'-Deoxy-B-D-ribofuranosyl)imidazole 5'-monophosphate (dImMP2-). International Journal of Chemistry Research, 9(9, SI):2050-2063.
DOI: https://doi.org/10.1002/cbdv.201100437

Synthesis and Acid–Base Properties of an Imidazole-Containing Nucleotide Analog, 1-(2′-Deoxy-β-D-ribofuranosyl)imidazole 5′-Monophosphate ($dImMP^{2-}$)

by **Nicole Megger**[a]), **Silke Johannsen**[b]), **Jens Müller***[a]), and **Roland K. O. Sigel***[b])

[a]) Institute of Inorganic and Analytical Chemistry, University of Münster, Corrensstrasse 28/30, D-48149 Münster (phone: +49 251 83 36006; fax: +49 251 83 36007; e-mail: mueller.j@uni-muenster.de)
[b]) Institute of Inorganic Chemistry, University of Zurich, Winterthurerstrasse 190, CH-8057 Zürich (phone: +41 44 635 4652; fax: +41 44 635 6802; e-mail: roland.sigel@aci.uzh.ch)

Deletion of the substituted pyrimidine ring in purine-2′-deoxynucleoside 5′-monophosphates leads to the artificial nucleotide analog $dImMP^{2-}$. This analog can be incorporated into DNA to yield, upon addition of Ag^+ ions, a molecular wire. Here, we measured the acidity constants of $H_2(dImMP)^{\pm}$ having one proton at N(3) and one at the PO_3^{2-} group by potentiometric pH titrations in aqueous solution. The micro acidity constants show that N(3) is somewhat more basic than PO_3^{2-} and, consequently, the $(H\cdot dImMP)^-$ tautomer with the proton at N(3) dominates to *ca.* 75%. The calculated micro acidity constants are confirmed by ^{31}P- and ^1H-NMR chemical shifts. The assembled data allow many quantitative comparisons, *e.g.*, the N(3)-protonated and thus positively charged imidazole residue facilitates deprotonation of the $P(O)_2(OH)^-$ group by 0.3 p*K* units. Information on the intrinsic site basicities also allows predictions about metal-ion binding; *e.g.*, Mg^{2+} and Mn^{2+} will primarily coordinate to the phosphate group, whereas Ni^{2+} and Cu^{2+} will preferably bind to N(3). Macrochelate formation for these metal ions is also predicted. The micro acidity constant for $N(3)H^+$ deprotonation in the $(H\cdot dImMP\cdot H)^{\pm}$ species (pk_a 6.46) and the M^{n+}-binding properties are of relevance for understanding the behavior of dImMP units present in DNA hairpins and metalated duplexes.

Introduction. – Nucleotide analogs receive much attention [1], *e.g.*, as (potential) drugs [2][3], as probes for enzymatic reactions [1][4], or as intermediates in biosynthetic pathways. A member of the latter category is the 5-amino-1*H*-imidazole ribonucleotide which is essential for the biosynthesis of thiamine [5–7], but also for the metabolism of purine mononucleotides [8] (*Fig. 1*, $dAMP^{2-}$, $dIMP^{2-}$, and $dGMP^{2-}$ [9][10]). Consequently, synthetic routes leading to the biosynthetic precursor 5-amino-1*H*-imidazole ribonucleotide have been developed [11]. However, despite the evident relationship to purine nucleotides, the unsubstituted imidazole ribonucleotide, being the product of a formal removal of the annelated pyrimidine ring (*Fig. 1*), has not been studied. This is also true for its 2′-deoxy derivative, $dImMP^{2-}$.

The nucleotide analog $dImMP^{2-}$ has recently been incorporated into a short DNA strand which, upon addition of Ag^+, gives rise to special structures like metalated duplexes [12]. At the same time, in the absence of Ag^+, the protonation state of the imidazole bases strongly affects local structures [13][14]. To rationalize these NMR solution structures and to interrelate them with the acid–base and metal-ion-binding behavior of the DNA analog, we have synthesized $dImMP^{2-}$ (*Fig. 1*) and studied its acid–base properties. A detailed study of the acidity constants of this nucleotide is

© 2012 Verlag Helvetica Chimica Acta AG, Zürich

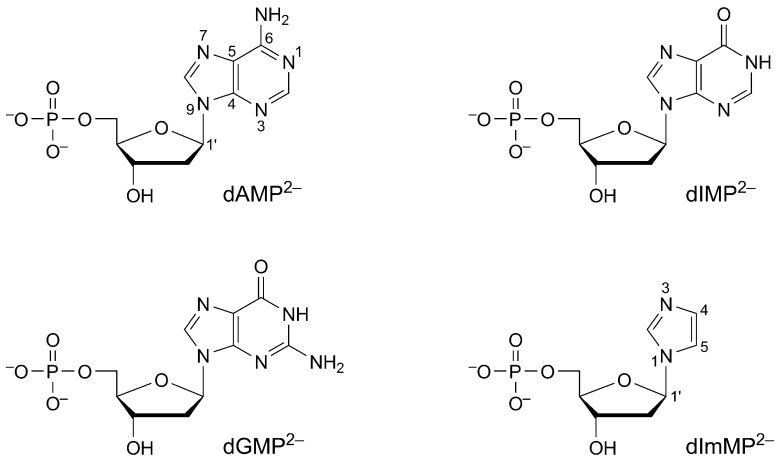

Fig. 1. *Chemical structures of the purine nucleotides 2′-deoxyadenosine 5′-monophosphate* ($dAMP^{2-}$), *2′-deoxyinosine 5′-monophosphate* ($dIMP^{2-}$), *and 2′-deoxyguanosine 5′-monophosphate* ($dGMP^{2-}$), *in comparison with the structure of 1-(2′-deoxy-β-*D*-ribofuranosyl)-1*H*-imidazole 5′-monophosphate* ($dImMP^{2-}$)

highly important, because it represents an example for a system comprising two protonable sites (here, imidazole and phosphate) with very similar proton affinities that directly influence each other. The determination of these properties now allows a general prediction of the metal-ion-binding properties of $dImMP^{2-}$ and their comparison with those of the purine nucleotides.

Results and Discussion. – 1. *Synthesis of dImMP*$^{2-}$. The 1*H*-imidazole nucleoside **1** was synthesized according to published methods [15] from 2-deoxy-D-ribose, which was first converted into *Hoffer*'s chloro sugar [16] so that the artificial nucleobase imidazole could be added in a second step *via* replacement of the Cl-atom (*Scheme*). Removal of the protecting groups led to the free nucleoside which was converted to the corresponding nucleotide by the addition of $POCl_3$ in $PO(OMe)_3$, followed by an aqueous workup. It was found that the phosphorylation of compound **1** resulted in the formation of two products, namely the desired 5′-monophosphate **2a** as well as the undesired 3′,5′-bisphosphate **2b** (*Scheme*).

Scheme. *Synthetic Route to dImMP*$^{2-}$ (**2a**), *Starting from Commercially Available 2-Deoxy-*D*-ribose*

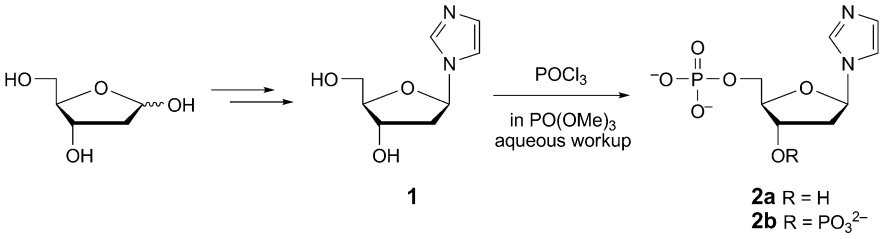

Compounds **2a** and **2b** were identified by mass spectrometry. Due to the lack of absorptivity above 200 nm, HPLC with UV detection of the purified analytes was not the method of choice for the purification of the nucleotide. Instead, the two products were separated by column chromatography ($KMnO_4$ was used to visualize the product spots on the TLCs) as a result of their different R_f values (0.12 for the monophosphate, 0.02 for the bisphosphate, TLC conditions: SiO_2, ^{i}PrOH/H_2O/NH_3 31:6:6).

2. *Potentiometric pH Titrations of H_2(dImMP)$^\pm$.* dImMP^{2-} (*Fig. 1*) can accept three protons, *i.e.*, two at the phosphate group and one at the imidazole moiety. The primary proton from the diprotonated phosphate group is certainly lost with $pK_a < 1$. Based on the structural similarity with H_3(dGMP)$^+$ (*Fig. 1*), which carries a proton at N(7) facilitating the release of the primary proton, one may assume that $pK^H_{H_3(dImMP)} \approx pK^H_{H_3(dGMP)} = 0.35 \pm 0.2$ [17]. Two further deprotonation reactions occur at the monoprotonated phosphate group and the also monoprotonated imidazole residue, giving rise to the following two deprotonation equilibria:

$$H_2(dImMP)^\pm \rightleftharpoons H(ImMP)^- + H^+ \quad (1a)$$

$$K^H_{H_2(dImMP)} = [H(dImMP)^-][H^+]/[H_2(dImMP)^\pm] \quad (1b)$$

$$H(dImMP)^- \rightleftharpoons dImMP^{2-} + H^+ \quad (2a)$$

$$K^H_{H(dImMP)} = [dImMP^{2-}][H^+]/[H(dImMP)^-] \quad (2b)$$

No other equilibria are expected in the physiological pH range because *i*) N(1) of imidazole is blocked by the sugar moiety, and *ii*) $pK_a = 12.5$ for the *cis*-arrangement of the 2′- and 3′-OH groups as present in a ribose residue [18]. For a 2′-deoxyribose residue, one may conclude that $pK_a > 13$ for the remaining 3′-OH group, because a 2′,3′-dihydroxy arrangement favors deprotonation of one of the two OH groups due to intramolecular H-bond formation in the resulting anion [18].

The acidity constants defined in *Eqns. 1b* and *2b* were determined by potentiometric pH titrations and are compiled in *Table 1* together with the data for some related systems [9][19–31], including 1-methyl-1*H*-imidazole (MeIm; *Entry 5*) and 2-deoxyribose 5-monophosphate (dRibMP^{2-}; *Entry 2*). The acidity constants of H(dRibMP)$^-$ and H(MeIm)$^+$ are not very far apart from each other ($\Delta pK_a = 0.9$), but the imidazole residue is clearly somewhat more basic compared to the phosphate group.

In accordance with the above observation is the reasoning that the first constant for the deprotonation of H_2(dImMP)$^\pm$, *i.e.*, $pK^H_{H_2(dImMP)} = 5.85 \pm 0.03$, is determined mainly by the release of the proton from the $P(O)_2(OH)^-$ group, and the second one, $pK^H_{H(dImMP)} = 6.88 \pm 0.04$, by the deprotonation of the monoprotonated imidazole residue. These two acidity constants differ by *ca.* 1 pK_a unit, meaning that the buffer regions of the two acid–base residues of dImMP^{2-} overlap. Consequently, the acidity constants determined by potentiometric pH titrations as given in *Table 1* are macro constants that quantify the overall situation for the H_2(dImMP)$^\pm$ species, but describe only approximately that for the individual proton-binding sites (see *Sect. 3*).

The distribution curves of the various species as they result from the macro acidity constants are shown in *Fig. 2*. These curves confirm the overlapping buffer regions. A

Table 1. *Negative Logarithms of the Acidity Constants of H_2(dImMP)$^{\pm}$ (Eqns. 1 and 2), together with the Corresponding Data for Some Related Compounds*[a])[b])

Entry	Acid	pK_a Values for the sites		Ref.
		$P(O)_2(OH)^-$	$N(3)H^+$	
1	$MeOPO_2(OH)^-$	6.36 ± 0.01		[9][20]
2[c])	H(dRibMP)$^-$	6.31 ± 0.07		–[c])
3[d])	H_2(dImMP)$^{\pm}$	5.85 ± 0.03	6.88 ± 0.04	–[d])
4[e])	H(dRibIm)$^+$		6.09 ± 0.07	–[e])
5[f])	H(MeIm)$^+$		7.20 ± 0.02	[25]
6[f])[g])	H(dRibBzIm)$^+$		4.29 ± 0.06	–[g])
7[f])	H(MeBzIm)$^+$		5.67 ± 0.01	[28]
8	H_2(dGMP)$^{\pm}$	6.29 ± 0.01	2.69 ± 0.03[h])	[29]
9	H(dGuo)$^+$		2.30 ± 0.04[h])	[30][31]

[a]) The constants were determined by potentiometric pH titrations (except *Entries 4* and *6*) in aqueous solution (25°C; I = 0.1M, $NaNO_3$). The so-called practical (or mixed) constants [19] are listed (see also *Exper. Part*). [b]) The error limits given are *three times* the standard error of the mean value (3σ) or the sum of the probable systematic errors, whichever is larger; error limits for any derived data, including ΔpK_a values (see also text), were calculated according to *Gaussian* error-propagation principles. [c]) The acidity constant of monoprotonated 5-ribose monophosphate ($RibMP^{2-}$) ($pK^H_{H(RibMP)} = 6.24 \pm 0.01$) [21] can be transformed to that of 2-deoxyribose 5-monophosphate ($dRibMP^{2-}$) by adding 0.07 ± 0.07 log units. This correction term follows from results obtained for a series of nucleoside 5′-monophosphates and 2′-deoxynucleoside 5′-monophosphates [22] and reflects the effect due to the replacement of OH by H at C(2) of the ribose residue (for details, see [22]). [d]) This work. [e]) At 25°C and natural ionic strength (*i.e.*, $I \approx 0.02$M), the value for monoprotonated 1-(2′-deoxy-β-D-ribofuranosyl)-1*H*-imidazole (dRibIm), $pK^H_{H(dRibIm)} = 6.01 \pm 0.05$, was determined by ^{1}H-NMR chemical-shift recordings [15]. It is well-known that, for this type of compounds [23], the pK_a values increase slightly with increasing *I:* for example, for monoprotonated imidazole (Im) the $pK^H_{H(Im)}$ values are 7.05 ± 0.01 at I = 0.1M [24] and 7.13 ± 0.01 at I = 0.5M [25] hold, and for monoprotonated pyridine (Py) the $pK^H_{H(Py)}$ values are 5.26 ± 0.01 (I = 0.1M) [26] and 5.34 ± 0.02 (I = 0.5M) [27]. We assume that the effect for H(dRibIm)$^+$ is similar and add 0.08 pK unit with the generous error limit of ± 0.05 to the mentioned value. The estimated result for I = 0.1M, *i.e.*, $pK^H_{H(dRibIm)} = (6.01 \pm 0.05) + (0.08 \pm 0.05) = 6.09 \pm 0.07$, is listed above. [f]) MeIm = 1-methyl-1*H*-imidazole; MeBzIm = 1-methyl-1*H*-benzimidazole; dRibBzIm = 1-(2′-deoxy-β-D-ribofuranosyl)-1*H*-benzimidazole. [g]) In analogy to *Entry 4*, based on the pK_a value of H(dRibBzIm)$^+$ as determined by ^{1}H-NMR spectroscopy at natural ionic strength (4.21 ± 0.03) [32], the same value is estimated to amount to 4.29 ± 0.06 at I = 0.1M. [h]) This value refers to the $N(7)H^+$ unit of the guanine residue, *i.e.*, the site corresponding to N(3) of an imidazole residue (*Fig. 1*). Deprotonation of the N(1)H unit in $dGMP^{2-}$ and in dGuo occurs with $pK^H_{dGMP} = 9.56 \pm 0.02$ (*cf.* [29]) and $pK^H_{dGuo} = 9.24 \pm 0.03$ [30][31], respectively.

consequence of this property is that the H(dImMP)$^-$ species reaches a formation degree of only *ca.* 62% (see also *Sect. 3*). Below, we will first discuss the various acidity constants collected in *Table 1*.

Table 1 allows many comparisons, but a few need to be emphasized:

i) The pK_a values for monoprotonated methyl monophosphate (*Entry 1*) and 2′-deoxyribose-5′-monophosphate (*Entry 2*) are astonishingly similar. This indicates that the solvation of the phosphate group in both compounds is quite similar.

ii) The above observation contrasts with *Entries 4* and *5:* here replacement of a Me group by the 2′-deoxyribose moiety at N(1) of 1*H*-imidazole leads to a significant

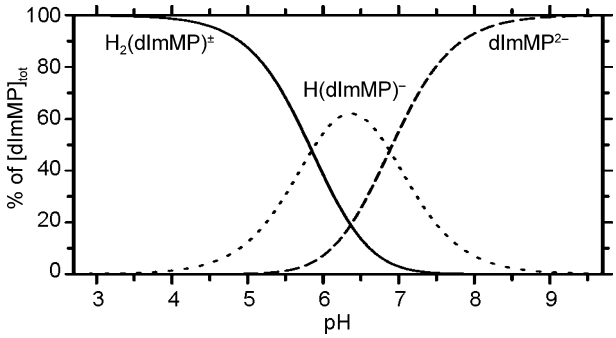

Fig. 2. *Effect of pH on the concentration of the species present in an aqueous solution of dImMP*$^{2-}$ (25°; $I = 0.1$M, $NaNO_3$). The calculations are based on the acidity constants compiled in *Table 1*, and the results are plotted as the percentage of the total dImMP present.

acidification of the N(3)H$^+$ unit. In this case, the substituents seem to affect solvation, and one is thus inclined to speculate that the 5′-OH group forms to some extent a H-bond with N(3), and that this facilitates deprotonation of N(3)H$^+$. Related H-bonds have recently also been suggested for xanthosine 5′-monophosphate [33].

iii) It is expected that the monoprotonated phosphate group in H_2(dImMP)$^{\pm}$ (*Entry 3*) is more acidic than that in H(dRibMP)$^-$ (*Entry 2*), because the positively charged monoprotonated imidazole residue should facilitate deprotonation of the $P(O)_2(OH)^-$ group.

iv) Along the same line, the deprotonation of the N(3)H$^+$ unit in H(dImMP)$^-$ (*Entry 3*, *Column 4*) is inhibited, compared to the same deprotonation reaction in H(dRibIm)$^+$ (*Entry 4*), because of the presence of the negatively charged PO_3^{2-} residue (for a detailed analysis, *cf. Sect. 3* and *Fig. 3*).

v) Annelation of 1-methyl-1*H*-imidazole (*Entry 5*) leading to 1-methyl-1*H*-benzimidazole (*Entry 7*) leads to a drop in basicity of N(3) by *ca.* 1.5 p*K* units. In analogy, the benzimidazole 2′-deoxyribonucleoside dRibBzIm (*Entry 6*) is more basic than its imidazole analog (*Entry 4*) by *ca.* 1.8 p*K* units. This contrasts sharply with the annelation of dImMP^{2-} (*Entry 3*) by a pyrimidine ring giving dGMP^{2-} (*Entry 8*). In the latter case, the basicity of N(7) drops by more than 4 p*K* units. Clearly, the electron-withdrawing effect of the substituted pyrimidine ring (*Fig. 1*) is much larger than that of a benzene ring.

Some further related points need to be discussed in the next section in the context of the evaluation of the micro acidity constants.

3. *Micro-Acidity-Constant Scheme for H_2(dImMP)$^{\pm}$*. For a quantification of the individual acid–base sites in dImMP^{2-}, it is necessary to determine the so-called micro acidity constants [34][35]. These micro acidity constants are connected with the macro acidity constants as shown in *Fig. 3*. The scheme contains four micro acidity constants, but there are only three independent equations (lower part of *Fig. 3*), which interlink the macro with the micro acidity constants. Hence, one of these micro acidity constants needs to be experimentally determined or estimated to be able to complete the scheme.

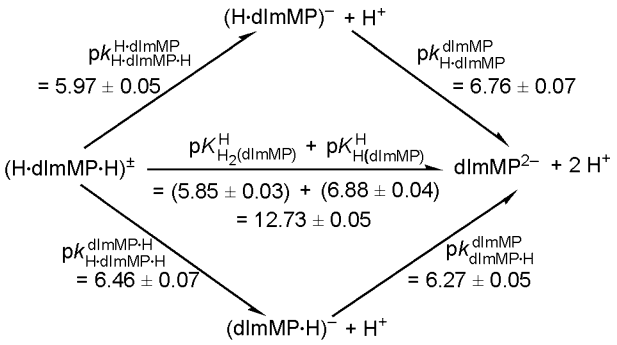

$$K^{H}_{H_2(dImMP)} = k^{H\cdot dImMP}_{H\cdot dImMP\cdot H} + k^{dImMP\cdot H}_{H\cdot dImMP\cdot H} \quad (a)$$

$$\frac{1}{K^{H}_{H(dImMP)}} = \frac{1}{k^{dImMP}_{H\cdot dImMP}} + \frac{1}{k^{dImMP}_{dImMP\cdot H}} \quad (b)$$

$$K^{H}_{H_2(dImMP)} \cdot K^{H}_{H(dImMP)} = k^{H\cdot dImMP}_{H\cdot dImMP\cdot H} \cdot k^{dImMP}_{H\cdot dImMP} = k^{dImMP\cdot H}_{H\cdot dImMP\cdot H} \cdot k^{dImMP}_{dImMP\cdot H} \quad (c)$$

Fig. 3. *Equilibrium scheme for (H·dImMP·H)±, also often formulated as H_2(dImMP)±, and its deprotonation to dImMP2− defining the micro acidity constants* (k)*, and showing their interrelation with the measured macro acidity constants* (K) *and the connection between the two tautomers (H · dImMP)⁻ and (dImMP · H)⁻ and the other species present.* In (H · dImMP)⁻, the proton is at N(3) of the imidazole residue, and in (dImMP · H)⁻ it is bound to the phosphate residue. In (H · dImMP · H)±, both sites are protonated. The arrows indicate the direction for which the acidity constants are defined. Use of the acidity constants determined for a series of 2′-deoxynucleoside 5′-monophosphates (dNMP)2−, *i.e.*, p$K^{H}_{H(dNMP)}$ of = 6.27 ± 0.05 [22], for the deprotonation of $P(O)_2(OH)^-$ in (dImMP · H)⁻, *i.e.*, for the micro acidity constant p$k^{dImMP}_{dImMP\cdot H}$ (lower pathway of the scheme at the right), permits calculation of the other micro acidity constants with equations *a*, *b*, and *c* given in the lower part of the above figure. The error limits are defined in *Footnote b* of *Table 1*.

In a recent study, it has been shown for a series of 2′-deoxynucleoside 5′-monophosphates (dNMP2−) that they all have p$K^{H}_{H(dNMP)}$ = 6.27 ± 0.05 [22]. Consequently, it is reasonable to assume that the micro acidity constant p$k^{dImMP}_{dImMP\cdot H}$ is well represented by the mentioned value, because, in the second deprotonation step in the lower pathway in *Fig. 3*, the imidazole residue is uncharged, as it is the case in the H(dNMP)⁻ species. Insertion of the mentioned acidity constant in the lower pathway at the right side of the scheme allows now calculation of the other three micro acidity constants by application of the equations given in the lower part of *Fig. 3*. These calculated constants are inserted at their corresponding positions in the scheme.

These micro acidity constants permit calculation of the ratio between the tautomers [34] with either a protonated imidazole residue or a monoprotonated phosphate residue for the H(dImMP)⁻ species (*Eqn. 3*):

$$R = \frac{[(\mathrm{H}\cdot\mathrm{dImMP})^-]}{[(\mathrm{dImMP}\cdot\mathrm{H})^-]} \tag{3a}$$

$$= \frac{k^{\mathrm{H\cdot dImMP}}_{\mathrm{H\cdot dImMP\cdot H}}}{k^{\mathrm{dImMP\cdot H}}_{\mathrm{H\cdot dImMP\cdot H}}} = \frac{10^{-(5.97\pm0.05)}}{10^{-(6.46\pm0.07)}} \tag{3b}$$

$$= 10^{(0.49\pm0.09)} = 3.09\pm0.64 \tag{3c}$$

$$= \frac{76}{24}\left(\frac{79}{21};\frac{71}{29}\right) \tag{3d}$$

Indeed, this result (the upper and lower limits are given in parentheses) establishes that both monoprotonated tautomeric species occur in appreciable amounts. Nevertheless, the imidazole residue is somewhat more basic than the phosphate group as already indicated in *Sect. 2*. Consequently, the imidazole-protonated species (at N(3)), $(\mathrm{H}\cdot\mathrm{dImMP})^-$, dominates with a formation degree of *ca.* 75%, whereas the phosphate-protonated minor species, $(\mathrm{dImMP}\cdot\mathrm{H})^-$, forms at *ca.* 25%. It should be noted that the ratio *R* given above is independent of the pH of the solution, because it represents an intramolecular equilibrium. Thus, a given amount of $\mathrm{H(dImMP)}^-$, large or small, will always be present in the ratio of *ca.* 75 to 25%.

With the micro acidity constants of *Fig. 3* at hand, several additional conclusions are possible; for example:

i) In $\mathrm{H(dRibIm)}^+$, the proton from the $\mathrm{N(3)H}^+$ site is released with $\mathrm{p}K^{\mathrm{H}}_{\mathrm{H(dRibIm)}} = 6.09\pm0.07$ (*Table 1*, *Entry 4*). In accordance with point *iv*) in *Sect. 2*, the presence of a negatively charged $\mathrm{P(O)_2(OH)}^-$ group retards the release of the $\mathrm{N(3)H}^+$ proton in $(\mathrm{H\cdot ImMP\cdot H})^\pm$ by $\Delta\mathrm{p}K_\mathrm{a} = \mathrm{p}k^{\mathrm{dImMP\cdot H}}_{\mathrm{H\cdot dImMP\cdot H}} - \mathrm{p}K^{\mathrm{H}}_{\mathrm{H(dRibIm)}} = (6.46\pm0.07) - (6.09\pm0.07) = 0.37\pm0.10$. This difference in acidity is within the error limits identical with that of the $\mathrm{H_2(dGMP)}^\pm/\mathrm{H(dGuo)}^+$ pair (*Table 1*; *Entries 8* and *9*), *i.e.*, $\Delta\mathrm{p}K_\mathrm{a} = \mathrm{p}K^{\mathrm{H}}_{\mathrm{H_2(dGMP)}} - \mathrm{p}K^{\mathrm{H}}_{\mathrm{H(dGuo)}} = (2.69\pm0.03) - (2.30\pm0.04) = 0.39\pm0.05$. Note that the steric conditions concur in both comparisons (*Fig. 1*), and consequently the $\Delta\mathrm{p}K_\mathrm{a}$ values are identical despite the large differences in the absolute size of the acidity constants considered.

ii) Instead of taking into account the effect of the $\mathrm{P(O)_2(OH)}^-$ group on the release of a proton from the $\mathrm{N(3)H}^+/\mathrm{N(7)H}^+$ site, one may also look at the effect of $\mathrm{N(3)H}^+$ on the release of a proton from the $\mathrm{P(O)_2(OH)}^-$ group by comparing $\mathrm{H(dRibMP)}^-$ with $\mathrm{H_2(dImMP)}^\pm$, *i.e.*, $\Delta\mathrm{p}K_\mathrm{a} = \mathrm{p}K^{\mathrm{H}}_{\mathrm{H(dRibMP)}} - \mathrm{p}k^{\mathrm{H\cdot dImMP}}_{\mathrm{H\cdot dImMP\cdot H}} = (6.31\pm0.07) - (5.97\pm0.05) = 0.34\pm0.09$. This difference is within the error limits identical with those discussed in *i*. This needs to be the case, because *Coulomb* effects are always reciprocal, and in all instances considered here the effects of singly charged sites are compared.

The outcome of the quantitative comparisons described above is very comforting because it establishes the internal consistency of the acidity constants assembled in *Table 1* and *Fig. 3*. The retarding effect of a *twofold* negatively charged $\mathrm{PO_3^{2-}}$ group on the deprotonation of $\mathrm{N(3)H}^+$ in $(\mathrm{H\cdot dImMP})^-$ is larger as the comparison with $\mathrm{H(dRibIm)}^+$ shows: $\mathrm{p}k^{\mathrm{dImMP}}_{\mathrm{H\cdot dImMP}} - \mathrm{p}K^{\mathrm{H}}_{\mathrm{H(dRibIm)}} = (6.76\pm0.07) - (6.09\pm0.07) = 0.67\pm0.10$. Evidently, the effect has approximately doubled as one would expect.

4. *^{31}P-NMR Spectroscopy.* Determination of the chemical shift of ^{31}P, δ(P), in dependence on pD in D_2O should reflect the acid–base properties of the phosphate group. Indeed, such a dependence is observed (*Fig. 4*).

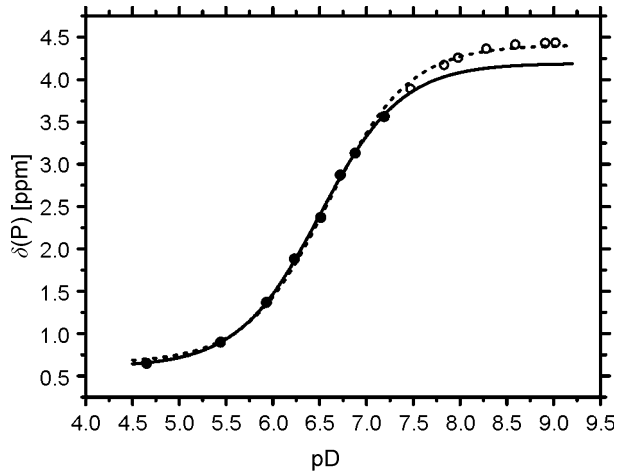

Fig. 4. *Variation of the chemical shift $\delta(^{31}P)$ of the phosphate group of dImMP^{2-}* (1.8 mM) *in dependence on pD* (25 °C; I = 0.12M, $NaClO_4$; see also *Exper. Part*). The dotted curve represents the calculated best fit through all experimental data, whereas, for the calculation of the solid curve, only the data points up to pD 6.88 were used.

An evaluation of the experimental data depicted in *Fig. 4* shows that they all fit on the dotted line. However, as described above (*Fig. 2*), the deprotonation reactions of H_2(dImMP)$^{\pm}$ and H(dImMP)$^-$ overlap. To minimize the influence of the deprotonation reaction of the monoprotonated imidazole residue on the deprotonation reaction of the monoprotonated phosphate residue, we first deleted the seven data points at pD > 7.2 in the evaluation. Indeed, the pK_a value of 6.58 ± 0.06 derived from all ^{31}P-NMR chemical shifts recorded in D_2O dropped to 6.49 ± 0.06 upon deletion of these data points. To validate the situation further, the data points at pD 7.19, 6.88, and 6.72 were also systematically deleted in the fitting process to give the pK_{a/D_2O} values of 6.50 ± 0.10, 6.51 ± 0.15, and 6.42 ± 0.12, respectively. We consider pK_{a/D_2O} = 6.50 ± 0.10 as the best result, which is based on the seven data points up to pD 6.88 (solid line in *Fig. 4*), because at this pD the protonated imidazole residue is still present to *ca.* 80 %.

Transformation [36] of the latter mentioned constant (valid in D_2O) to H_2O as solvent by applying *Eqn. 4* leads to pK_{a/H_2O} = 5.96 ± 0.10 (3σ).

$$pK_{a/H_2O} = (pK_{a/D_2O} - 0.45)/1.015 \quad (4)$$

This value is within the error limits identical with the micro acidity constant given at the left in the upper pathway of *Fig. 3*, thus verifying this method. This result allows two conclusions:

i) By deleting a number of data points in *Fig. 4* (see the solid line), it is indeed possible to determine the micro acidity constant for the deprotonation of the phosphate group under conditions where the imidazole group is protonated.

ii) The agreement between the micro acidity constant as determined by ^{31}P-NMR experiments (5.96 ± 0.10) and that calculated (5.97 ± 0.05) for $pk^{H\cdot dImMP}_{H\cdot dImMP\cdot H}$ in *Fig. 3* shows that our previous assumption, *i.e.*, $pK^{H}_{H(dNMP)} = 6.27 \pm 0.05 = pk^{dImMP}_{dImMP\cdot H}$, as stated in *Sect. 3*, is justified. Further verification of all data is provided by the excellent fit of all 15 ^{31}P-NMR data points (*Fig. 4*) by using the two micro acidity constants given in the upper pathway of *Fig. 3* (see Fig. S1[1])).

With the mentioned micro acidity constant experimentally confirmed, the effect of a protonated imidazole residue on the deprotonation of the monoprotonated phosphate group in $H_2(dImMP)^{\pm}$ can now be quantified. The corresponding acidification follows from *Eqn. 5:*

$$\Delta pK_a = pk^{dImMP}_{dImMP\cdot H} - pk^{H\cdot dImMP}_{H\cdot dImMP\cdot H} \quad (5a)$$

$$= (6.27 \pm 0.05) - (5.97 \pm 0.05) \quad (5b)$$

$$= 0.30 \pm 0.07 \quad (5c)$$

This result is most reasonable and in agreement with the related observations discussed in *i* and *ii* of *Sect. 3*.

To conclude, potentiometric pH titrations allow the determination of acidity constants in an exact manner, but this method does not provide any direct information about the sites from which the protons are released. Therefore, it is satisfying to see that the site attributions made earlier in *Sect. 2* and *3*, which were solely based on the comparison of constants, are confirmed by the NMR shift experiments described above as well as by those to follow below.

5. *^{1}H-NMR Studies of dImMP^{2-}*. One expects that the chemical shifts (δ(H)) of H–C(2), H–C(4), and H–C(5) of 1*H*-imidazole would be affected by the protonation/deprotonation of N(3). Indeed, with decreasing pD downfield shifts are observed as it is commonly the case (*Fig. 5*), whereby δ(H) of H–C(2) is most strongly affected [22][37][38].

A curve-fitting of the experimental data for each of the three H-atoms (*Fig. 5*) yields a single pK_a value only, the average of which gives $pK_a = 7.13 \pm 0.12$. The corresponding acidity constant valid for H_2O (*Eqn. 4*) is $pK_{a/H_2O} = 6.58 \pm 0.12$. A comparison of this value with the macro acidity constants given on the horizontal arrow in *Fig. 3* shows that it is *ca.* 0.3 pK_a units below $pK^{H}_{H(dImMP)} = 6.88$. More importantly, this value from the ^{1}H-NMR shift experiments is also below $pk^{dImMP}_{H\cdot dImMP} = 6.76 \pm 0.07$ but above $pk^{dImMP\cdot H}_{H\cdot dImMP\cdot H} = 6.46 \pm 0.07$. This implies that the value from the ^{1}H-NMR experiments does not reflect any of the micro acidity constants, a situation that cannot be improved easily for the three H-atoms considered. The deletion of data points, as done in the ^{31}P-NMR experiments (*Fig. 4*), is of course also a possibility. Because the chemical-shift differences for H–C(4) and H–C(5) are too small to allow for a reliable evaluation, we concentrated on the chemical shifts of H–C(2): if one deletes the four data points at pH < 6.4, and then systematically also the points at pD 6.51, 6.58, 6.72, and 7.19, one obtains the pK_a values of 7.19 ± 0.05, 7.22 ± 0.05, 7.20 ± 0.06, and $7.15 \pm$

[1]) *Supplementary Material* may be obtained upon request from the authors.

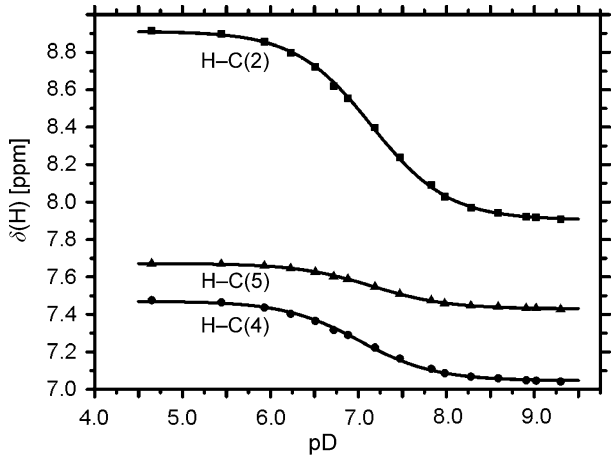

Fig. 5. *Variation of the chemical shift δ(H) for the H-atoms of the imidazole residue in dImMP*$^{2-}$ (1.8 mM) *in dependence on pD* (25°; $I = 0.12$M, $NaClO_4$; see also *Exper. Part*). The solid curves are the calculated best fits of the experimental data using the micro acidity constants $pk^{D\cdot dImMP}_{D\cdot dImMP\cdot D} = 6.51 \pm 0.05$ and $pk^{dImMP}_{D\cdot dImMP} = 7.31 \pm 0.07$.

0.10, respectively. With regard to the micro acidity constant $pk^{dImMP}_{D\cdot dImMP}$, we consider as the best result 7.22 ± 0.05 (the corresponding fit is shown in Fig. S2[1])). Transformation of this value to an aqueous solution (H_2O) with *Eqn. 4* gives $pk^{dImMP}_{H\cdot dImMP} = 6.67 \pm 0.05$. Comparison of this result with the corresponding value in *Fig. 3* (upper pathway at the right), *i.e.*, $pk^{dImMP}_{H\cdot dImMP} = 6.76 \pm 0.07$, shows that the agreement is reasonable, though not completely satisfying. However, this is understandable because deprotonation of the imidazole residue takes place under the influence of an increasing twofold negative charge at the phosphate group. Hence, here we have the stronger $2-/1+$ *Coulomb* interaction, whereas, previously in *Sect. 4*, it was a $1-/1+$ interaction only.

The validity of the chemical-shift change for all three H-atoms can be checked in the following way: we used the micro acidity constants given in the upper pathway of *Fig. 3* and converted these with *Eqn. 4* to the pk_a values valid for D_2O as solvent, $pk^{D\cdot dImMP}_{D\cdot dImMP\cdot D} = 6.51 \pm 0.05$ and $pk^{dImMP}_{D\cdot dImMP} = 7.31 \pm 0.07$. Indeed, with these two micro acidity constants, the experimental data for all three protons can be fitted excellently as the solid curves in *Fig. 5* displays. Use of the macro acidity constants does not lead to such satisfactory fits as is obvious from the error limits, which are twice as large (*cf. Table 2* and Table S1[1])).

The described fitting procedure, using the micro acidity constants, also provides the chemical-shift data for the $(H\cdot dImMP\cdot H)^{\pm}$, $(H\cdot dImMP)^{-}$, and $dImMP^{2-}$ species (*Table 2*).

From the $\Delta\delta_1$ and $\Delta\delta_2$ values listed in *Columns 5* and *6* of *Table 2*, it becomes clear that the chemical shifts are largely governed by the deprotonation of $N(3)H^+$ in $(H\cdot dImMP)^{-}$, as the effect of the $P(O)_2(OH)^{-}$ deprotonation in $(H\cdot dImMP\cdot H)^{\pm}$ is much smaller. This result is in accordance with the larger distances of the phosphate group to the monitored protons.

Table 2. *^{1}H-NMR Chemical Shifts* [ppm] *of the Protonated, i.e., Deuterated, and the Free Forms of dImMP^{2-}*[a])[b])

H-Atom	$\delta((D \cdot dImMP \cdot D)^{\pm})$	$\delta((D \cdot dImMP)^{-})$	$\delta(dImMP^{2-})$	$\Delta\delta_2$	$\Delta\delta_1$
H–C(2)	8.919(12)	8.643(20)	7.902(8)	0.276(23)	0.741(21)
H–C(4)	7.477(6)	7.300(10)	7.043(4)	0.177(12)	0.257(11)
H–C(5)	7.674(4)	7.610(6)	7.428(3)	0.064(7)	0.182(8)

[a]) The chemical shifts were calculated with the transformed micro acidity constants (*Fig. 3*, upper pathway; application of *Eqn. 4*) based on the experiments in D_2O that yield the data plotted in *Fig. 5* (25 °C; I = 0.12M, $NaClO_4$). The chemical-shift differences, $\Delta\delta$, resulting from increasing deprotonation of the species are also listed, *i.e.*, $\Delta\delta_2 = \delta((D \cdot dImMP \cdot D)^{\pm}) - \delta((D \cdot dImMP)^{-})$ and $\Delta\delta_1 = \delta((D \cdot dImMP)^{-}) - \delta(dImMP^{2-})$. [b]) The specified error ranges for the calculated chemical shifts (δ) and the chemical-shift differences ($\Delta\delta$) are *three times* the standard deviations (3σ) in each case.

Conclusions. – From the right hand part of *Fig. 3*, it is evident that the imidazole residue in $dImMP^{2-}$ is by *ca.* 0.5 pK units more basic than the phosphate residue in the same molecule. Consequently, *ca.* 75% (*Eqn. 3*) of the $H(dImMP)^{-}$ species carry the proton at the imidazole residue and exist as the $(H \cdot dImMP)^{-}$ tautomer. The second tautomer, $(dImMP \cdot H)^{-}$, is a minor species, but, with a formation degree of *ca.* 25%, it is not negligible.

These acid–base properties allow the prediction, based on known metal-ion affinities of imidazoles [25] and phosphates [39], that the primary binding site for complex formation of metal ions such as Ca^{2+}, Mg^{2+}, and even Mn^{2+} is the phosphate residue. In contrast, for metal ions such as Co^{2+}, Ni^{2+}, Cu^{2+}, or Zn^{2+} the imidazole residue is the primary binding site. In agreement with the results observed for AMP^{2-}, also macrochelate formation occurs [40]. In fact, one expects that macrochelate formation is more pronounced in the case of this artificial nucleotide, $dImMP^{2-}$, due to the higher basicity of the endocyclic N-site compared to the M(AMP) complexes. Zn(dImMP) and Cd(dImMP) promise to be especially interesting, because the involved metal ions have a rather similar affinity towards the imidazole and phosphate groups; this then should give rise to equilibria between three isomeric complexes [33][35], *i.e.*, macrochelates as well as monodentate-bound species coordinated either to the imidazole or the phosphate residue.

Finally, these results help to understand the different solution structures [12–14] determined by NMR spectroscopy at various pH values of a DNA sequence comprising several imidazole residues besides mainly natural nucleosides. Such artificial oligonucleotides can be metalated in their helix center with, *e.g.*, Ag^{+} [12]. In the absence of metal ions, these nucleic acids adopt a hairpin conformation, and the protonation/deprotonation properties of these are currently being investigated. Generally, information on the relationship between structures and perturbed pK_a values of residues is of great importance in order to understand local structures and acid–base catalysis in ribozymes [41]. Considering that a nucleotide moiety within a nucleic acid involves a singly charged phosphodiester bridge, which is of no relevance regarding proton binding in the physiological pH range, the basicity of the imidazole residue becomes crucial for the artificial nucleotide. This basicity should be well represented by the $(dImMP \cdot H)^{-}$ species, *i.e.*, by the micro acidity constant $pk^{dImMP \cdot H}_{H \cdot dImMP \cdot H} = 6.46 \pm 0.07$

(*Fig. 3*; lower pathway at the left). In other words, this value represents the basis for comparisons of the acid–base properties of the imidazole residues in the different hairpin structures.

Financial support by the *ERAnet-Chemistry*, the *Swiss National Science Foundation* (200021_124834 to *R. K. O. S.*), *Marie Heim-Vögtlin Fellowship* (to *S. J.*), the *Deutsche Forschungsgemeinschaft* (MU1750/1-3 and MU1750/2-1 to *J. M.*), the *Swiss State Secretariat for Education and Research* (*R. K. O. S.*), *COST D39*, and the Universities of Zürich and Münster is gratefully acknowledged, as are helpful suggestions provided by Professor Dr. *H. Sigel* from the University of Basel, Switzerland. *R. K. O. S.* is a recipient of an *ERC Starting Grant 2010*.

Experimental Part

General. The reagents used for the potentiometric pH titrations and the NMR experiments were the same as employed previously [22].

Potentiometric pH Titrations and Determination of the Acidity Constants of H_2(dImMP)$^{\pm}$. The pH titrations were carried out with an *E536* potentiograph connected to an *E665* dosimat and a *6.0253.100 Aquatrode-plus* combined macro glass electrode (all from *Metrohm AG*, CH-Herisau). The buffer solns. of pH 4.00 and 7.00 were also purchased from *Metrohm AG*, and the one of pH 9.21 was from *Mettler-Toledo GmbH* (CH-Schwerzenbach). All buffer solns. are based on standard reference materials (SRM) of the US National Institute of Science and Technology (NIST). The acidity constants determined at $I=$ 0.1M ($NaNO_3$) and 25°C are so-called practical mixed or *Brønsted* constants [19], which may be converted to the corresponding concentration constants by subtracting 0.02 from the measured pK_a values [19]. It should be emphasized that the ionic product of water (K_w) does not enter into our calculations, because the differences in NaOH consumption between solns. with and without the nucleotide analogs are evaluated. The acidity constants $K^H_{H_2(dImMP)}$ and $K^H_{H(dImMP)}$ of H_2(dImMP)$^{\pm}$ were determined by titrating 30 ml of aq. 0.42 mM HNO_3 (25°C; $I=0.1$M, $NaNO_3$) in the presence and absence of 0.1 mM dImMP^{2-} under N_2 with up to 1 ml of 0.02M NaOH. To save the scarce nucleotide, after each titration the pair of solns. was adjusted again to the initial pH of *ca.* 4.3 by adding a small volume (*ca.* 0.13 ml) of 0.1M HNO_3, and then the titrations were repeated. The exper. data were evaluated by means of a curve-fitting procedure using a *Newton–Gauss* nonlinear least-squares program that utilized the difference in NaOH consumption between the aforementioned pairs of titrations, *i.e.*, with and without the nucleotide, at increments of 0.1 pH units. The acidity constants were calculated within the pH range of 4.3 to 7.5, which corresponds to a neutralization degree of *ca.* 97% for the equilibrium $H_2(dImMP)^{\pm} \rightleftharpoons H(dImMP)^-$ and that of *ca.* 80% for the equilibrium $H(dImMP)^- \rightleftharpoons (dImMP)^{2-}$ (*Fig. 2*). The final acidity constants are the averages of six measurements with three independent pairs of titration solutions.

^{31}P- and ^{1}H-NMR Experiments. ^{31}P-, ^{13}C-, and ^{1}H-NMR spectra of dImMP (1.8 mM) in D_2O, in dependence on pD, were recorded on *Bruker AV III* and *AV2-400* spectrometers (400 MHz) with a QNP probe at 25°C and $I=0.12$M ($NaClO_4$). Chemical shifts for ^{31}P recordings were referenced to the external standard 85 % H_3PO_4 (H_2O, $\delta=0$ ppm), and ^{1}H recordings to the external standard 3-(trimethylsilyl)-propane-1-sulfonate (D_2O, $\delta=0$ ppm), resp. The pD of the solns. was adjusted by dotting with a glass stick using relatively conc. DNO_3 and NaOD solns. The actual pD was then measured by means of a *Hamilton Minitrode* glass electrode (*Hamilton AG*, CH-Bonaduz) connected to a *Metrohm 605* digital pH meter (*Metrohm AG*, CH-Herisau). The final pD values of the solns. were obtained by adding 0.40 to the pH-meter reading [42][43]. The exper. data were analyzed by means of the *Newton–Gauss* nonlinear least-squares method. Results were obtained with the aid of a computer-based curve-fitting program, which was based on the general equation published previously [37][44][45]. This equation relates the observed chemical shift, δ_{obsd}, with the p$K^H_{H_2(dImMP)}$ and p$K^H_{H(dImMP)}$ values, and the chemical shifts for the species H_2(dImMP)$^{\pm}$, H(dImMP)$^-$, and dImMP^{2-}. The ^{1}H-NMR signals of dImMP^{2-} were assigned in analogy to those of dRibIm [15].

dImMP^{2-} (**2a**). The synthetic route to this imidazole nucleotide is outlined in the *Scheme*. To a soln. of the imidazole nucleoside **1** [15] (1.41 g, 7.65 mmol; dried *in vacuo* at r.t. for 30 min) in $PO(OMe)_3$

(50 ml; solubilized by slight heating), cooled in an ice bath, $POCl_3$ (781 µl, 8.42 mmol, 1.1 equiv.) was added. After stirring for 1 h at 0 °C, the reaction was quenched by the addition of ice (200 ml), and the mixture was neutralized with aq. NH_3. The solvent was removed by evaporation *in vacuo*, and the crude product was purified by column chromatography (SiO_2, ^{i}PrOH/H_2O/NH_3 31:6:6) to yield **2a** (866 mg, 34%). Hygroscopic white solid. The side product **2b** (3′,5′-bisphosphate) was identified by mass spectrometry and not further characterized. ^{1}H-NMR (D_2O, pD 7.25): 8.54 (*s*, H–C(2)); 7.60 (*s*, H–C(5)); 7.29 (*s*, H–C(4)); 6.27 (*t*, H–C(1′)); 4.64 (*m*, H–C(3′)); 4.24 (*m*, H–C(4′)); 3.97 (*m*, CH_2(5′)); 2.65 (*m*, H–C(2′)); 2.55 (*m*, H–C(2′)). ^{13}C-NMR (D_2O, pD 7.25): 135.3 (C(2)); 124.0 (C(5)); 118.7 (C(4)); 87.6 (C(4′)); 86.6 (C(1′)); 71.0 (C(3′)); 63.8 (C(5′)); 40.5 (C(2′)). ^{31}P-NMR (D_2O, pD 7.25): 2.54. HR-MS: 265.05792 ($[M+H]^+$, $C_8H_{14}N_2O_6P$; calc. 265.0584). Anal. calc. for $C_8H_{13}N_2O_6P \cdot 1.5\ NH_3 \cdot 2.5\ H_2O$ (334.76): C 28.70, H 6.77, N 14.64; found: C 28.96, H 5.92, N 14.75. Copies of the ^{1}H-, ^{13}C-, and ^{31}P-NMR spectra of **2a** in D_2O at pD 7.25 are available as the *Supplementary Material* (Fig. S3[1]).

REFERENCES

[1] R. K. O. Sigel, H. Sigel, *Met. Ions Life Sci.* **2007**, *2*, 109.
[2] H. Sigel, *Chem. Soc. Rev.* **2004**, *33*, 191.
[3] A. Holý, I. Votruba, M. Masojídková, G. Andrei, R. Snoeck, L. Naesens, E. De Clercq, J. Balzarini, *J. Med. Chem.* **2002**, *45*, 1918.
[4] R. K. O. Sigel, B. Song, H. Sigel, *J. Am. Chem. Soc.* **1997**, *119*, 744.
[5] B. G. Lawhorn, R. A. Mehl, T. P. Begley, *Org. Biomol. Chem.* **2004**, *2*, 2538.
[6] M. J. Dougherty, D. M. Downs, *J. Bacteriol.* **2004**, *186*, 4034.
[7] A. Chatterjee, Y. Li, Y. Zhang, T. L. Grove, M. Lee, C. Krebs, S. J. Booker, T. P. Begley, E. S. Ealick, *Nat. Chem. Biol.* **2008**, *4*, 758.
[8] M. Dougherty, D. M. Downs, *J. Bacteriol.* **2003**, *185*, 332.
[9] C. P. Da Costa, D. Krajewska, A. Okruszek, W. J. Stec, H. Sigel, *J. Biol. Inorg. Chem.* **2002**, *7*, 405.
[10] K. Aoki, *Met. Ions Biol. Syst.* **1996**, *32*, 91.
[11] M. J. Humphries, C. A. Ramsden, *Synthesis* **1999**, 985.
[12] S. Johannsen, N. Megger, D. Böhme, R. K. O. Sigel, J. Müller, *Nat. Chem.* **2010**, *2*, 229.
[13] S. Johannsen, D. Böhme, N. Düpre, J. Müller, R. K. O. Sigel, 'NMR solution structure of modified DNA containing imidazole nucleosides at basic pH', PDB ID 2K69, doi: 10.2210/pdb2k69/pdb.
[14] S. Johannsen, D. Böhme, N. Düpre, J. Müller, R. K. O. Sigel, 'NMR solution structure of modified DNA containing imidazole nucleosides at acidic pH', PDB ID 2K67, doi: 10.2210/pdb2k67/pdb.
[15] J. Müller, D. Böhme, P. Lax, M. Morell Cerdà, M. Roitzsch, *Chem. – Eur. J.* **2005**, *11*, 6246.
[16] M. Hoffer, *Chem. Ber.* **1960**, *93*, 2777.
[17] B. Knobloch, H. Sigel, A. Okruszek, R. K. O. Sigel, *Org. Biomol. Chem.* **2006**, *4*, 1085.
[18] B. Lippert, *Prog. Inorg. Chem.* **2005**, *54*, 385.
[19] H. Sigel, A. D. Zuberbühler, O. Yamauchi, *Anal. Chim. Acta* **1991**, *255*, 63.
[20] A. Saha, N. Saha, L.-n. Ji, J. Zhao, F. Gregan, S. A. A. Sajadi, B. Song, H. Sigel, *J. Biol. Inorg. Chem.* **1996**, *1*, 231.
[21] S. S. Massoud, H. Sigel, *Inorg. Chem.* **1988**, *27*, 1447.
[22] A. Mucha, B. Knobloch, M. Jeżowska-Bojczuk, H. Kozłowski, R. K. O. Sigel, *Chem. – Eur. J.* **2008**, *14*, 6663.
[23] L.-n. Ji, N. A. Corfù, H. Sigel, *J. Chem. Soc., Dalton Trans.* **1991**, 1367.
[24] L.-n. Ji, N. A. Corfù, H. Sigel, *Inorg. Chim. Acta* **1993**, *206*, 215.
[25] L. E. Kapinos, B. Song, H. Sigel, *Inorg. Chim. Acta* **1998**, *280*, 50.
[26] D. Banerjea, T. A. Kaden, H. Sigel, *Inorg. Chem.* **1981**, *20*, 2586.
[27] L. E. Kapinos, H. Sigel, *Inorg. Chim. Acta* **2002**, *337*, 131.
[28] L. E. Kapinos, B. Song, H. Sigel, *Chem. – Eur. J.* **1999**, *5*, 1794.
[29] B. Song, H. Sigel, *Inorg. Chem.* **1998**, *37*, 2066.
[30] H. Sigel, B. Song, G. Oswald, B. Lippert, *Chem. – Eur. J.* **1998**, *4*, 1053.
[31] B. Song, J. Zhao, R. Griesser, C. Meiser, H. Sigel, B. Lippert, *Chem. – Eur. J.* **1999**, *5*, 2374.

[32] J. Müller, D. Böhme, N. Düpre, M. Mehring, F.-A. Polonius, *J. Inorg. Biochem.* **2007**, *101*, 470.
[33] H. Sigel, B. P. Operschall, R. Griesser, *Chem. Soc. Rev.* **2009**, *38*, 2465.
[34] B. Song, R. K. O. Sigel, H. Sigel, *Chem. – Eur. J.* **1997**, *3*, 29.
[35] H. Sigel, S. S. Massoud, B. Song, R. Griesser, B. Knobloch, B. P. Operschall, *Chem. – Eur. J.* **2006**, *12*, 8106.
[36] R. B. Martin, *Science* **1963**, *139*, 1198.
[37] R. K. O. Sigel, E. Freisinger, B. Lippert, *J. Biol. Inorg. Chem.* **2000**, *5*, 287.
[38] W. Brüning, E. Freisinger, M. Sabat, R. K. O. Sigel, B. Lippert, *Chem. – Eur. J.* **2002**, *8*, 4681.
[39] H. Sigel, L. E. Kapinos, *Coord. Chem. Rev.* **2000**, *200–202*, 563.
[40] E. M. Bianchi, S. A. A. Sajadi, B. Song, H. Sigel, *Chem. – Eur. J.* **2003**, *9*, 881.
[41] R. K. O. Sigel, A. M. Pyle, *Chem. Rev.* **2007**, *107*, 97.
[42] P. K. Glasoe, F. A. Long, *J. Phys. Chem.* **1960**, *64*, 188.
[43] R. Lumry, E. L. Smith, R. R. Glantz, *J. Am. Chem. Soc.* **1951**, *73*, 4330.
[44] R. Tribolet, H. Sigel, *Eur. J. Biochem.* **1987**, *163*, 353.
[45] W. Brüning, R. K. O. Sigel, E. Freisinger, B. Lippert, *Angew. Chem., Int. Ed.* **2001**, *40*, 3397.

Received December 28, 2011